

## Single and competitive adsorption of V-EDTA and Ni-EDTA complexes onto activated carbon: response surface optimization, kinetic, equilibrium, and thermodynamic studies<sup>†</sup>

Mohammad Poorbaba, Mansooreh Soleimani\*

Department of Chemical Engineering, Amirkabir University of Technology (Tehran Polytechnic), No. 350, Hafez Ave., P.O. Box: 1591634311, Tehran, Iran, emails: soleimanim@aut.ac.ir (M. Soleimani), m.poorbaba@aut.ac.ir (M. Poorbaba)

Received 21 March 2020; Accepted 30 September 2020

### ABSTRACT

Extraction with an aqueous solution of ethylenediaminetetraacetic acid (EDTA) is a convenient method to recover vanadium and nickel from their secondary resources, such as spent catalysts and fly ash. In this paper, V-EDTA and Ni-EDTA complexes were adsorbed from aqueous phase using activated carbon (NAC) in single and competitive adsorption systems. The operational parameters were metal concentrations ( $C_{i,M}$ ), EDTA concentration ( $L/M$ ), solution pH ( $pH_i$ ), and adsorbent dosage ( $C_{Ads}$ ). At single adsorption of these complexes, the maximum  $q$  was obtained 15.39 mg g<sup>-1</sup> for V-EDTA and 15.82 mg g<sup>-1</sup> for Ni-EDTA. Competitive studies were conducted at three concentrations of the initial metal. At the following conditions,  $C_{i,V} = 120$  mg L<sup>-1</sup>,  $C_{i,Ni} = 40$  mg L<sup>-1</sup>,  $pH_i = 3.0$ , and  $C_{Ads} = 12$  g L<sup>-1</sup>, the ratio of adsorbed vanadium to nickel ( $q_V/q_{Ni}$ ) was obtained 11.84 after 7 h. Likewise, a modified pseudo-second-order kinetic model was given for the first time to describe the whole competitive adsorption process. Moreover, adsorptions of free EDTA and Na<sup>+</sup> at competitive experiments were investigated. The results of equilibrium and kinetics experiments illustrated that the pseudo-second-order kinetic model and Freundlich and Dubinin–Radushkevich isotherms could describe experimental data well.

**Keywords:** Vanadium; Nickel; Ethylenediaminetetraacetic acid; Adsorption; Optimization

### 1. Introduction

Vanadium and nickel are two toxic heavy metals that have many applications in industries. The known oxidation states of vanadium are -1 to +5 that the states +3, +4, and +5 are the most common [1]. For nickel, the states -1 to +4 are known while the +2 state is the most common [2,3]. These two heavy metals have extensive usage in many industries such as metalworking, steel, glass, ceramic, textile, photography, and producing pigments, catalysts, and some kind of batteries [1,4–12]. Due to the toxicity and useful applications of these two heavy metals, it is necessary to remove and reuse them.

There are several methods to recover vanadium and nickel from their secondary resources such as heavy cuts of crude oil [4], spent catalysts [13–16], and fly ash produced in heavy fuel power plants [17]. Chemical deposition, extraction, membrane filtration, adsorption, and distillation are some effective methods to be mentioned [4,18–21]. Among the mentioned methods, extraction with organic acids is taken into consideration in this study. The extraction with organic acids is taken place in milder operational conditions in comparison to the inorganic ones [16].

Among various kinds of inorganic acids, ethylenediaminetetraacetic acid (EDTA) is a strong chelating agent extract vanadium and nickel from their secondary resources

\* Corresponding author.

<sup>†</sup> This research did not receive any specific grant from funding agencies in the public, commercial, or not-for-profit sectors.

[4,15,17]. After the extraction process by the aqueous solution of EDTA, it is a desire to move out V-EDTA and Ni-EDTA compounds from the aqueous solution. According to the non-biodegradability of EDTA [22], this action has benefits that reuse the water for the extraction process cycle and vanadium and nickel in relevant industries. In this work, adsorption of V-EDTA and Ni-EDTA from EDTA aqueous solution is investigated due to the adsorption method benefits that are its low cost, flexibility, and easy operation [6]. An activated carbon was used as an adsorbent because of its efficiency to adsorb the organic compounds [23–25].

According to the literature review, there was no similar work about the adsorption of V-EDTA complex and its competitive adsorption in the presence of Ni-EDTA complex. This work and our previous study [26] are trying to investigate the influences of operational parameters to design and operate a cyclic process of vanadium and nickel extraction from their secondary resources. The main aims of this study are as follows:

- To optimize the operational parameters including metal concentrations, EDTA concentration, solution pH, and adsorbent dosage in adsorption of V-EDTA and Ni-EDTA complexes individually and find a well-describing model based on the operational parameters for each one.
- To study the kinetics and equilibrium of each metal-ligand system and describe the experimental data with a proper model.
- To study the competitive adsorption of V-EDTA and Ni-EDTA systems in the optimum operational conditions derived from the individual adsorption experiments.
- To obtain the best modified kinetic model for the first time to describe the whole competitive adsorption process.

## 2. Materials and methods

### 2.1. Materials

A commercial activated carbon produced by Norit Company (GAC 830 W) was used as an adsorbent and named NAC in this investigation. Extra pure grade of salts  $V_2O_5$ ,  $NiN_2O_6 \cdot 6H_2O$ , and  $C_{10}H_{14}N_2Na_2O_8 \cdot 2H_2O$  were used to prepare stock solutions of V-EDTA and Ni-EDTA (2,000 mg L<sup>-1</sup> based on metals). To adjust the initial pH of the metal-ligand containing solutions, 1.0 N NaOH or 1.0 N HNO<sub>3</sub> were used. pH<sub>pzc</sub> characterization of NAC adsorbent was measured by using NaCl solution. All chemicals were purchased from Merck Company. Deionized water with specific conductance 18.2 MΩ cm at 25°C and total organic carbon (TOC) 6 ppb produced by Milli-Q water purification system was used to prepare all solutions.

### 2.2. Characterization of adsorbent

Some characteristics of NAC such as adequate particle size, iodine number, apparent density, ball-pan hardness, moisture, and ash content were measured using the following standard test methods, respectively:

- ASTM D 2862-97, D 4607-94, D 2854-96, D 3802-79, D 2867-99, and D 2866-94.

The porous textures of NAC, including specific surface area, average pore radius, and pore volume, were analyzed by applying the Brunauer–Emmett–Teller (BET) method on N<sub>2</sub> adsorption at 77 K [27]. These measurements were done before and after the adsorption process by using BEL Belsor-mini instrument. Surface functional groups of NAC and their changes after the adsorption process were determined by studying the Fourier transform infrared (FTIR) spectrum. This analysis was done with NEXUS Nicolet 670 instrument. The point of zero charge pH (pH<sub>pzc</sub>) was measured using several NaCl solutions with a concentration of 0.1 N at different pH. The procedure is available in reference [28].

### 2.3. Experimental procedures

At the first step, adsorption of V-EDTA and Ni-EDTA individually on NAC were investigated. In the second step, the competitive adsorption of them was studied at optimum conditions derived from the first step.

To study the adsorption of V-EDTA and Ni-EDTA individually onto NAC, the response surface method (RSM) was used to design the experiments. In these tests, the experimental design was performed to investigate the influence of main operating variables, including initial metal concentration, EDTA concentration, initial pH, and adsorbent dosage for each system. The adsorption experiments were done in 50 mL of a solution containing metal-ligand components. The initial pH of the solutions was adjusted by adding 1.0 N NaOH or 1.0 N HNO<sub>3</sub>. The pH was controlled by a digital pH meter with an accuracy of 0.1 (Genway, model 3345). A shaker incubator (N-BIOTEK, model NB-205) was used to agitate the mixtures at 25°C. The agitation speed and adsorption time were set 230 rpm, and 4 h, respectively. In the end, the adsorbents were separated using Whatman no. 1 filter papers, and metal concentration in each solution was determined with ICP-OES (Varian, model 730-ES Axial) analysis instrument. The adsorbent capacity,  $q_M$  (mg g<sup>-1</sup>), was chosen as a response and calculated from Eq. (1).

$$q_M = \frac{C_{i,M} - C_{f,M}}{C_{Ads}} \quad (1)$$

where  $C_{i,M}$  and  $C_{f,M}$  are the initial and final concentration of metal (mg L<sup>-1</sup>), and  $C_{Ads}$  is the adsorbent dosage (g L<sup>-1</sup>), respectively.

Competitive adsorption experiments were investigated kinetically. Operating conditions were selected based on the optimum operating conditions obtained from the individual adsorption systems. Accordingly, the initial pH and adsorbent dosage were set 3.0 and 12 g L<sup>-1</sup>, respectively. The ligand to the metal molar ratio ( $L/M$  ratio) that indicates EDTA concentration was set 1 in Ni-EDTA stock solution, but in V-EDTA stock solution, it was set 3. It was desired to investigate NAC performance in selective adsorption of metal-ligand components in the presence of free EDTA and Na. The complex of V-EDTA or Ni-EDTA is 1:1, which means that 1 mol of vanadium or nickel reacts with 1 mol of EDTA to form 1 mol of V-EDTA or Ni-EDTA complex [29,30]. At  $L/M$  ratio equals 1, there is no free EDTA in solution, but at other amounts greater than 1, free EDTA will appear in the solution.

To determine the initial concentrations of V-EDTA and Ni-EDTA at competitive experiments, previous works were considered [17]. Accordingly, the ratio of initial vanadium concentration to nickel concentration was set three in competitive experiments, and three series of experiments were done as follows:

- $C_{i,V} = 120 \text{ mg L}^{-1}$ ,  $C_{i,Ni} = 40 \text{ mg L}^{-1}$
- $C_{i,V} = 40 \text{ mg L}^{-1}$ ,  $C_{i,Ni} = 120 \text{ mg L}^{-1}$
- $C_{i,V} = 120 \text{ mg L}^{-1}$ ,  $C_{i,Ni} = 120 \text{ mg L}^{-1}$

where  $C_{i,V}$  and  $C_{i,Ni}$  are the initial vanadium concentration and the nickel concentration, respectively. To perform these experiments, 50 mL of containing metal-ligand solution was contacted at 25°C to the adsorbents at different contact times (20–420 min). After each time, the metal concentrations were measured and adsorbent capacity was calculated by Eq. (1) and the adsorption percentage was determined by using Eq. (2).

$$\text{Metal Adsorption \%} = \frac{C_{i,M} - C_{f,M}}{C_{i,M}} \times 100 \quad (2)$$

It was required to measure the free EDTA and Na concentration in the competitive adsorption process. The concentration of free EDTA was measured by titration with 0.001 M ZnCl<sub>2</sub> solution in the presence of a buffer solution to keep the pH constant at 5.5 [31]. Xylenol orange (XO) was used to recognize the titration endpoint. The titration was finished when the color of the solution turns into purple-red that indicates forming of Zn-XO complex. To measure the concentration of Na, a flame photometer (Sherwood, model 410) was used. The adsorption percentage and adsorbent capacity of free EDTA and Na were calculated by using Eqs. (3) and (4), respectively.

$$\text{EDTA/Na Adsorption \%} = \frac{C_i - C_f}{C_i} \times 100 \quad (3)$$

$$q_{\text{EDTA/Na}} = \frac{C_i - C_f}{C_{\text{Ads}}} \quad (4)$$

where  $C_i$  and  $C_f$  are the concentrations of free EDTA or Na at the initial and end of the adsorption process (mmol L<sup>-1</sup>), respectively.

#### 2.4. Modeling and optimization procedures for non-competitive adsorption

In this work, experiments were designed by Design Expert software (version 8.0.6) from Stat-Ease Company. The central composite design (CCD) was used as a method of designing due to some advantages like its ability to fit the quadratic model and insensitive to missing data [26,32]. At CCD, the parameter alpha ( $\alpha$ ), which locates the star points, was set 1 due to limitations of the initial pH of the solutions, especially for Ni-EDTA system [30].

According to our previous work and literature review, four independent variables were selected as the operational factors. Metal concentrations ( $X_1$ ), EDTA concentration, which is defined as the molar ratio of EDTA (ligand) to metal called  $L/M$  ( $X_2$ ), initial pH of the solution ( $X_3$ ), and adsorbent dosage ( $X_4$ ). The ranges of these variables were defined based on previous investigations and listed in Table 1 for both V-EDTA and Ni-EDTA systems with their coded levels.

For each metal-ligand system, 30 experiments were done. The number of these experiments could be calculated from the relation  $2^K + 2K + 6$ , where  $K$  is a number of the independent variables [33]. As the RSM result, a model describing the adsorption of metal-ligand complex onto NAC has been reported. For this purpose, several models, including linear, quadratic, and cubic were tested. These models are shown in Eqs. (5)–(7), respectively [32,33]. The coefficient of the proper model was estimated by performing the least square method and the adsorption capacity was maximized by solving the regression model [32,33].

$$y = \beta_0 + \sum_{i=1}^4 \beta_i X_i \quad (5)$$

$$y = \beta_0 + \sum_{i=1}^4 \beta_i X_i + \sum_{i=1}^3 \sum_{j=i+1}^4 \beta_{ij} X_i X_j + \sum_{i=1}^4 \beta_{ii} X_i^2 \quad (6)$$

$$y = \beta_0 + \sum_{i=1}^4 \beta_i X_i + \sum_{i=1}^3 \sum_{j=i+1}^4 \beta_{ij} X_i X_j + \sum_{i=1}^4 \beta_{ii} X_i^2 + \sum_{i=1}^2 \sum_{j=i+1}^3 \sum_{k=i+2}^4 \beta_{ijk} X_i X_j X_k + \sum_{i=1}^4 \sum_{j=1, j \neq i}^4 \beta_{ijj} X_i X_j^2 + \sum_{i=1}^4 \beta_{iii} X_i^3 \quad (7)$$

Table 1  
Ranges and levels of RSM operational factors

Factors	Coded levels									
	- $\alpha$		-1		0		+1		+ $\alpha$	
	V-EDTA	Ni-EDTA	V-EDTA	Ni-EDTA	V-EDTA	Ni-EDTA	V-EDTA	Ni-EDTA	V-EDTA	Ni-EDTA
$X_1$ $C_{i,M}$ (mg L <sup>-1</sup> )	40	40	40	40	120	120	200	200	200	200
$X_2$ $L/M$	1	1	1	1	2	2	3	3	3	3
$X_3$ pH <sub>i</sub>	2.0	3.0	2.0	3.0	5.0	6.0	8.0	9.0	8.0	9.0
$X_4$ $C_{\text{Ads}}$ (g L <sup>-1</sup> )	2	2	2	2	7	7	12	12	12	12

where  $i$ ,  $j$ , and  $k$  are the index numbers and  $y$  is the system response means adsorbent capacity based on the metal adsorption.  $\beta_0$ ,  $\beta_i$ ,  $\beta_{ii}$ , and  $\beta_{iii}$  are the regression coefficient, linear effect, squared effect, and cubic effect terms, respectively.  $\beta_{ij}$  represents the interaction effect of the quadratic model. Similarly,  $\beta_{ijk}$  and  $\beta_{ijj}$  are the interaction effects of the cubic model.  $X_i$ ,  $X_j$ , and  $X_k$  indicate the coded independent variables.

### 2.5. Equilibrium studies

The equilibrium studies were carried out individually for adsorption of V-EDTA and Ni-EDTA onto NAC. The equilibrium adsorption of V-EDTA was investigated in our previous work in the following operational condition:

- initial vanadium concentration = 100–320 mg L<sup>-1</sup>, L/M ratio = 3, initial pH of the solutions = 2.0, adsorbent dosage = 12 g L<sup>-1</sup>, and temperature = 25°C–45°C [26].

In this paper, equilibrium adsorption of Ni-EDTA complex was investigated at different initial concentrations (60–360 mg L<sup>-1</sup> nickel), and temperatures (25°C, 35°C, and 45°C). The adsorbent dosage was set to 12 g L<sup>-1</sup>, and other operational parameters including L/M ratio, and initial pH were set to their optimum values derived from RSM analysis.

The mixtures containing 50 mL of Ni-EDTA solution and NAC were agitated at 230 rpm for 24 h in the orbital shaker incubator. After reaching the equilibrium, the mixtures were filtered, and the remaining solutions were analyzed for nickel concentration. The equilibrium adsorbent capacity,  $q_e$  (mg g<sup>-1</sup>), was found from Eq. (1) by replacing the final concentration as the equilibrium concentration.

### 2.6. Kinetic studies

In this step, the kinetics of individual V-EDTA and Ni-EDTA complex adsorption onto NAC were studied. The kinetic results of V-EDTA adsorption have been reported in our previous work [26]. However for Ni-EDTA complex, 50 mL of its solution with an initial concentration of 120 mg L<sup>-1</sup> was contacted with NAC at 25°C and 230 rpm at different time steps. The adsorbent dosage was set to 12 g L<sup>-1</sup>, and the values of L/M ratio and initial pH of the solution were set to their optimum values derived from the model predicted by RSM. The solution was filtered after each time step and analyzed for nickel concentration. The adsorbent capacity at each time step,  $q_t$  (mg g<sup>-1</sup>), could be calculated from Eq. (1) by replacing the final concentration as the concentration at time  $t$  (min).

## 3. Results and discussions

### 3.1. Characteristics of adsorbent

Some characteristics of NAC are reported in Table 2. The parameters such as total surface area, mean pore diameter, and total pore volume were measured after the adsorption process at optimum conditions of maximum adsorbent capacity,  $q_{\max}$  (mg g<sup>-1</sup>), for both V-EDTA and Ni-EDTA systems. The porous texture characteristics after the process are as follows:

Table 2  
Characterization of NAC before adsorption

Parameter	Value
Effective particle size (mm)	1.6
Iodine number (mg I <sub>2</sub> g <sup>-1</sup> )	950
Apparent density (g mL <sup>-1</sup> )	0.47
Ball-pan hardness (%)	95
Moisture (wt.%)	5
Ash content (wt.%)	12
pH <sub>pzc</sub>	8.3
Total surface area (m <sup>2</sup> g <sup>-1</sup> )	1,021.5
Mean pore diameter (nm)	2.073
Total pore volume (cm <sup>3</sup> g <sup>-1</sup> )	0.529

- At V-EDTA system: total surface area = 846.7 m<sup>2</sup> g<sup>-1</sup>, mean pore diameter = 2.141 nm, and total pore volume = 0.453 cm<sup>3</sup> g<sup>-1</sup>.
- At Ni-EDTA system: total surface area = 926.0 m<sup>2</sup> g<sup>-1</sup>, mean pore diameter = 2.247 nm, and total pore volume = 0.520 cm<sup>3</sup> g<sup>-1</sup>.

As expected, the total surface area of NAC was decreased after the adsorption process at both systems. However, the increase in mean pore diameters and a decrease in total pore volumes at both systems show that the adsorption of V-EDTA and Ni-EDTA complexes occurred in NAC micro pores.

The NAC functional groups were investigated by studying the FTIR spectra before and after the adsorption process in each system. This analysis was done for the adsorbents, which were used in optimum operational conditions. The obtained results were analyzed by using reference [34] and are illustrated at Fig. 1. According to the NAC spectra before the adsorption process, the O–H functional group is detected at a wide peak at 3,422 cm<sup>-1</sup>. By considering the C–O sharp peak at 1,089 cm<sup>-1</sup>, it could be concluded that the detected O–H belongs to alcohols or phenols. The peaks at 2,922 and 2,838 cm<sup>-1</sup> may point to stretching C–H in an alkane. The peak at 1,736 cm<sup>-1</sup> attributes to C=O functional group at an ester. It is probable that the peak at 1,623 cm<sup>-1</sup> attributes to a bending N–H in primary or secondary amides.

Several moderate peaks at the range of 1,300–1,600 cm<sup>-1</sup> may introduce the bending C–H groups in an alkane with bonds of –CH<sub>2</sub>– and –CH<sub>3</sub>. The existence of a rocking bending C–H in an alkane or aromatic can be seen at 798 cm<sup>-1</sup>. After the adsorption process, at the spectra of both V-EDTA and Ni-EDTA systems, a severe decrease in the intensity of O–H and C–O peaks is seen. It means that OH<sup>-</sup> was released into the solution during the adsorption process that the pH measurements prove this happening. At the spectra of V-EDTA and Ni-EDTA system, a sharp peak at 673 cm<sup>-1</sup> has appeared. This peak may belong to C–H functional group that was hidden in the before adsorption spectra.

### 3.2. Model analysis for non-competitive adsorption

By using CCD, 30 experiments for V-EDTA and Ni-EDTA systems were designed individually. Table 3

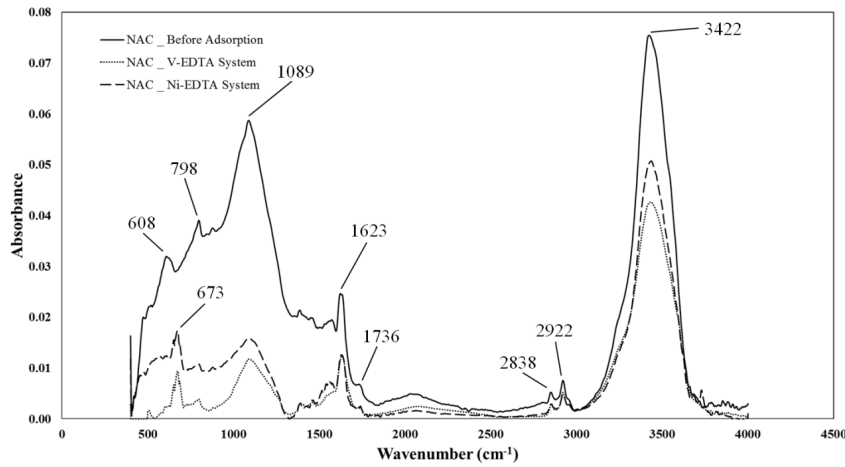


Fig. 1. FTIR spectra of NAC before and after of the adsorption for both metal-ligand systems.

Table 3  
Experiments of the central composite design including corresponding responses

Run	Independent variables in coded levels				Response $q$ (mg g <sup>-1</sup> )		Comment
	$X_1$	$X_2$	$X_3$	$X_4$	V-EDTA	Ni-EDTA	
1	-1	-1	-1	-1	7.02	6.35	FP
2	+1	+1	+1	+1	1.10	2.82	FP
3	0	+1	0	0	2.99	2.31	SP
4	+1	+1	-1	+1	9.22	4.11	FP
5	0	0	-1	0	8.71	4.30	SP
6	-1	+1	+1	-1	1.85	1.87	FP
7	+1	-1	-1	+1	11.51	6.45	FP
8	+1	-1	-1	-1	16.83	17.04	FP
9	0	0	0	0	2.67	2.28	CP
10	0	0	+1	0	0.68	0.43	SP
11	0	0	0	0	2.20	2.32	CP
12	-1	+1	-1	+1	3.28	1.22	FP
13	+1	+1	-1	-1	9.88	12.27	FP
14	0	0	0	-1	1.32	2.80	SP
15	-1	+1	-1	-1	7.04	2.15	FP
16	0	0	0	0	3.90	2.27	CP
17	0	-1	0	0	2.07	4.20	SP
18	0	0	0	0	3.04	1.91	CP
19	0	0	0	0	2.75	2.38	CP
20	0	0	0	+1	1.97	1.84	SP
21	-1	-1	+1	-1	2.53	5.55	FP
22	-1	-1	+1	+1	1.44	1.85	FP
23	+1	-1	+1	+1	2.09	3.81	FP
24	+1	+1	+1	-1	0.69	12.23	FP
25	-1	0	0	0	2.06	1.75	SP
26	-1	+1	+1	+1	1.27	1.56	FP
27	+1	-1	+1	-1	2.13	10.25	FP
28	0	0	0	0	2.71	3.12	CP
29	+1	0	0	0	3.61	4.66	SP
30	-1	-1	-1	+1	2.56	2.83	FP

FP: factorial point, SP: star point, CP: central point.

indicates the designed experiments with their operational conditions and corresponding response obtained from each experiment. According to the obtained results, the maximum  $q$  at V-EDTA and Ni-EDTA systems were 16.83 and 17.04 mg g<sup>-1</sup>, respectively. The maximum responses are approximately equal to each other, and both of them occurred at run 8. It could be concluded that the mechanism of the adsorption process for both systems is nearly the same.

To obtain the best model describing the experimental data, analysis of variance (ANOVA) was done. For each regression parameter,  $F$ -value and Prob. >  $F$  parameters were investigated. These two parameters at the ANOVA table demonstrate the importance and effectiveness of a model term. If the Prob. >  $F$  of a source is less than 0.0500, it could be concluded that it is a significant model term. Otherwise, if the Prob. >  $F$  is greater than 0.1000, the source is not a significant model term and should be omitted to improve the model accuracy [35]. Tables 4 and 5 are ANOVA results for V-EDTA and Ni-EDTA systems, respectively. According to these tables,  $F$ -value and Prob. >  $F$  of model source for V-EDTA system are 39.39 and <0.0001, and for Ni-EDTA system are 60.32 and <0.0001, respectively. These values demonstrate that both models describing V-EDTA and Ni-EDTA systems are significant. Also, the values of lack of fit indicate that lack of fitness of the models is not significant relative to their pure errors.

According to the ANOVA tables, there are some non-significant model terms that their Prob. >  $F$  values are greater than 0.1000, but they still exist in the models. These non-significant terms were not omitted. Because remaining them in the models will improve the model's adequacies. The final models for V-EDTA and Ni-EDTA systems in terms of substituted operational factors (Table 1) are written in Eqs. (8) and (9), respectively.

$$\text{Sqrt}(q_v) = 4.2097 - 0.0131X_1 - 0.3114X_2 - 0.3993X_3 - 0.2036X_4 + 9.3612E-03X_1X_2 - 5.1023E-03X_1X_3 + 2.7253E-03X_1X_4 + 9.5585E-03X_3X_4 + 1.0428E-04X_1^2 + 0.0369X_3^2 - 4.6330E-05X_1^2X_2 + 1.5340E-05X_1^2X_3 - 1.0113E-05X_1^2X_4 \tag{8}$$

$$\text{Sqrt}(q_{Ni}) = 4.3012 + 0.0171X_1 - 2.4840X_2 + 0.1616X_3 - 0.2170X_4 + 3.2428E-03X_1X_2 - 7.4463E-03X_1X_3 + 2.7456E-03X_1X_4 + 0.0354X_2X_3 + 0.0452X_2X_4 - 4.2004E-05X_1^2 + 0.3901X_2^2 - 2.8306E-04X_1X_2X_4 + 2.9478E-05X_1^2X_3 - 1.1567E-05X_1^2X_4 \tag{9}$$

According to Table 3, ratios of the maximum response to the minimum response in each metal-ligand system were higher than 10. So, a transformation is required to perform on the responses to obtain the proper model. By investigating the Box–Cox plots for each system, which were reported by Design Expert, the square root transform ( $\lambda = 0.5$ ) was selected.

The models reported for adsorption of metal-ligand components are non-complete cubic models. It was not possible to use a complete cubic model for each system because of non-adequacy and aliasing some model terms with each other. Likewise, the estimation of the least square parameters in the complete cubic model was not unique. The same non-complete cubic model has been used in our previous work [26] and Mehrabi's investigation [33].

The models statics including  $R^2$ , adjusted  $R^2$ , predicted  $R^2$ , adequate precision, and coefficient of variation have been reported in Table 6 for both systems. As it is evident, there are reasonable agreements between adjusted  $R^2$  and predicted  $R^2$  for both models. Also, adequate precision of the systems, which measures the adequacy of signal to noise, is greater than 4. It indicates an adequate signal

Table 4  
ANOVA table for V-EDTA adsorption

Source	Sum of squares	Degree of freedom	Mean square	F-value	Prob. > F
Model	18.170	13	1.400	39.39	<0.0001
$X_1$	1.350	1	1.350	38.14	<0.0001
$X_2$	0.042	1	0.042	1.18	0.2932
$X_3$	2.270	1	2.270	63.89	<0.0001
$X_4$	0.033	1	0.033	0.92	0.3510
$X_1X_2$	0.320	1	0.320	8.92	0.0087
$X_1X_3$	1.860	1	1.860	52.42	<0.0001
$X_1X_4$	0.230	1	0.230	6.41	0.0222
$X_3X_4$	0.330	1	0.330	9.27	0.0077
$X_1^2$	0.043	1	0.043	1.22	0.2853
$X_3^2$	0.380	1	0.380	10.70	0.0048
$X_1^2X_2$	0.160	1	0.160	4.40	0.0521
$X_1^2X_3$	0.150	1	0.150	4.35	0.0535
$X_1^2X_4$	0.190	1	0.190	5.25	0.0359
Residual	0.570	16	0.035	–	–
Lack of fit	0.430	11	0.039	1.48	0.3502
Pure error	0.130	5	0.027	–	–

Table 5  
ANOVA table for Ni-EDTA adsorption

Source	Sum of squares	Degree of freedom	Mean square	F-value	Prob. > F
Model	17.740	14	1.270	60.32	<0.0001
$X_1$	5.840	1	5.840	278.17	<0.0001
$X_2$	1.060	1	1.060	50.60	<0.0001
$X_3$	1.010	1	1.010	47.98	<0.0001
$X_4$	0.050	1	0.050	2.36	0.1450
$X_1X_2$	0.160	1	0.160	7.75	0.0139
$X_1X_3$	0.130	1	0.130	6.06	0.0264
$X_1X_4$	0.910	1	0.910	43.38	<0.0001
$X_2X_3$	0.180	1	0.180	8.60	0.0103
$X_2X_4$	0.051	1	0.051	2.42	0.1405
$X_1^2$	0.410	1	0.410	19.50	0.0005
$X_2^2$	0.520	1	0.520	24.95	0.0002
$X_1X_2X_4$	0.210	1	0.210	9.76	0.0070
$X_1^2X_3$	0.570	1	0.570	27.11	0.0001
$X_1^2X_4$	0.240	1	0.240	11.59	0.0039
Residual	0.320	15	0.021	–	–
Lack of fit	0.240	10	0.024	1.50	0.3431
Pure error	0.079	5	0.016	–	–

Table 6  
Models statics and constants

Model statics	Value	
	V-EDTA system	Ni-EDTA system
$R^2$	0.9697	0.9825
Adjusted $R^2$	0.9451	0.9663
Predicted $R^2$	0.8799	0.9176
Adequate precision	24.042	31.279
C.V.%	10.20	7.54

[36,37]. Moreover, the parameter specifies that the repeatability and precision of a model (C.V.%) has an acceptable value for both systems.

Comparing the experimental data with models prediction (Fig. 2) showed that the actual and predicted data are nearly the same. Finally, by considering all of the analysis done to examine the models, it could be claimed that the obtained models have a great ability to describe the design spaces.

### 3.3. Parameter optimization for non-competitive adsorption

The optimization of operational parameters was carried out to obtain the maximum capacity of NAC ( $q_M$ ). This numerical optimization was done with Design Expert. At the software optimization module, maximization of the  $q_M$  for both systems was set as the “goal,” and the status of the operational parameters were set to “in range” criterion.

The maximum  $q$  for vanadium adsorption at V-EDTA system was predicted 15.39 mg g<sup>-1</sup> by the model with a desirability value of 0.910 in the following conditions:

- $C_{i,V} = 200$  mg L<sup>-1</sup>,  $L/M = 1$ ,  $pH_i = 2.0$ , and  $C_{Ads} = 2$  g L<sup>-1</sup>.

Similarly, the maximum  $q$  for nickel adsorption at Ni-EDTA system was predicted 15.82 mg g<sup>-1</sup> by the model with a desirability value of 0.927 in the following conditions:

- $C_{i,Ni} = 200$  mg L<sup>-1</sup>,  $L/M = 1$ ,  $pH_i = 3.0$ , and  $C_{Ads} = 2$  g L<sup>-1</sup>.

The optimum results were tested by repeating the experiments to ensure their validity. The relative errors obtained from the verification experiments for V-EDTA and Ni-EDTA systems were only 8.6% and 8.7%, respectively.

### 3.4. Comparison the results with other researches

The comparison of the RSM optimum results with other similar works was carried out and tabulated in Table 7. Except for this work and our previous work, there is no study on adsorption of V-EDTA complex onto an adsorbent. There was also just one work that insignificantly investigated the Ni-EDTA adsorption onto a commercial activated carbon [30]. So, the results of this work are compared with other works that investigated the adsorption of vanadium and nickel metals in the absence of EDTA component. However, the obtained values for the adsorption of metal-ligand complex were in reasonable agreement with other studies.

At Bhattacharyya and Cheng's work [30], where Ni-EDTA adsorbed onto a commercial activated carbon, the operational conditions were as follows:

- $C_{i,Ni} = 50$  mg L<sup>-1</sup>,  $L/M = 1$ ,  $pH_i = 5.0$ , and  $C_{Ads} = 20$  g L<sup>-1</sup>. At these operational conditions, the  $q_{max}$  for Ni was reported 2.5 mg g<sup>-1</sup>, which is relatively low. In this paper, by optimizing the operational conditions, the  $q_{max}$  for Ni was increased to 15.82 mg g<sup>-1</sup> that has grown significantly.

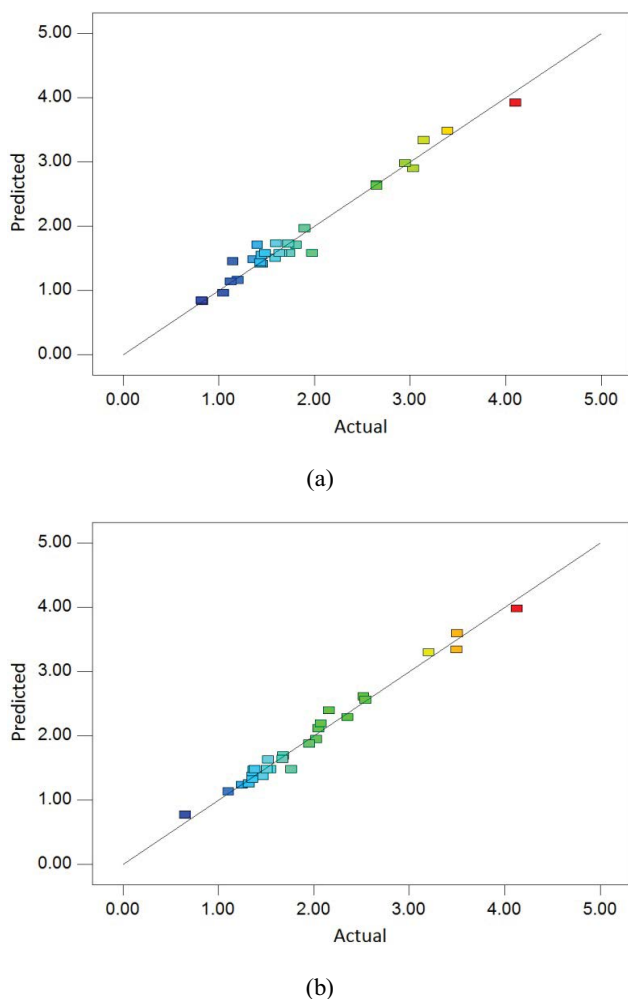


Fig. 2. Predicted vs. actual values plot for (a) V-EDTA and (b) Ni-EDTA system.

Table 7

Results of other works for vanadium and nickel adsorption

Adsorbent	$C_{i,M}$ (mg L <sup>-1</sup> )		pH <sub>i</sub>	$C_{Ads}$ (g L <sup>-1</sup> )	$q_{max}$ (mg g <sup>-1</sup> )		References
	V	Ni			V	Ni	
Commercial activated carbon	–	50.0	5.0	20.0	–	2.5	[30]
Modified clinoptilolite	–	5.9–5,869.3	1.0–12.0	10.0	–	528.2	[38]
EDTA functionalized silica	–	20.0–200.0	1.5–6.5	1.0	–	67.6	[39]
EDTA/DTPA functionalized silica gel	–	1.0–250.0	1.0–7.0	2.0–25.0	–	21.6	[40]
Modified activated carbon	–	25.0–700.0	2.0–10.0	3.3	–	166.7	[41]
Silylated clays	–	10.0–2,000.0	1.0–6.0	0.1–17.0	–	17.1	[42]
Modified tamarind fruit shell	5.0–50.0	–	2.0–8.0	0.5–5.0	45.9	–	[43]
Calcined Mg/Al hydrotalcite	50.0	–	2.0–9.0	0.2	230.0	–	[44]
Waste metal sludge	7.6–48.4	–	–	10.0	24.8	–	[45]
Commercial activated carbon	25.0–200.0	–	4.5	1.0	37.8	–	[6]
Fe modified activated carbon	25.0–200.0	–	4.5	1.0	119.0	–	
Protonated chitosan flakes	1.0–5.0	–	4.4–5.0	5.0	12.2	–	[18]
ZnCl <sub>2</sub> activated carbon	40.0–120.0	–	4.0–9.0	4.0	24.9	–	[46]
Commercial activated carbon	40.0–200.0	40.0–200.0	2.0–9.0	2.0–12.0	15.4	15.8	This work

### 3.5. Effects of operational parameters

In this paper, the influence of four operational parameters on adsorption of V-EDTA and Ni-EDTA individually onto NAC was investigated. Among these parameters, the initial concentration of adsorbates and adsorbent dosage have well-known influences on an adsorption process. At constant  $L/M$  ratio, by increasing the metal ion concentration, the concentration of metal-ligand complex will increase. This increase leads to an increase in the adsorption driving force, and greater amounts of metal-ligand complex will be adsorbed.

As the adsorbent dosage decreases, less of the adsorbate is adsorbed, and its concentration remains high, so the driving force in the adsorption process remains high too and it resulting an increasing  $q$  parameter. Nevertheless, not in this work, some adsorbents have unpredictable behaviors that influenced the adsorption process. Agglomeration and dissolving in the solution are some behaviors that could be mentioned [44,47].

According to the above, the optimum  $q$  occurred at the maximum value of initial metal concentration range, and the minimum value of adsorbent dosage range are defined in Table 1. Among the operational parameters, the  $L/M$  and initial pH are more important. For better physical justification of the EDTA concentration, the  $L/M$  ratio is replaced. It demonstrates the molar ratio of ligand (EDTA) to metal (V or Ni). Since the V-EDTA and Ni-EDTA complexes are 1:1, it means that one mole of EDTA and 1 mol of each metal are required to form one mole of metal-ligand complex [29,30], there was free EDTA in the solution at  $L/M$  values greater than 1. The existence of free EDTA has a negative influence on the adsorption of metal-ligand complex (the reason is explained in the following section). So at  $L/M = 1$ , there was no free EDTA in the solution, and the maximum  $q$  for both metal-ligand complexes occurred.

But, the most important operational parameter was initial pH of the solution. Because this factor sets the charge

of the metal-ligand complex, free EDTA component, and surface charge of NAC. The surface charge of NAC is positive when the solution pH is lower than its  $pH_{pzc}$  (8.3). So in almost all RSM experiments, the surface charge of NAC was positive, and anions had more tendencies to be adsorbed. At  $L/M$  ratios greater than 1, there were free EDTA species that their charges were changed by pH solution. At RSM experiments in which initial pH was in the range of 2.0–9.0, all EDTA compounds had negative charges. At the range of pH mentioned earlier, the dominant species of EDTA are  $H_3[EDTA]^-$ ,  $H_2[EDTA]^{2-}$ , and  $H[EDTA]^{3-}$  [48]. Due to the negative charge of EDTA species and positive charge of NAC surface, free EDTA was adsorbed with metal-ligand complex onto NAC and occupied some of the adsorbent active sites. Therefore, the existence of free EDTA in the solution decreases the adsorption of metal-ligand complex.

At weak acidic solutions, the dominant species of V-EDTA was  $VO_2[EDTA]^{3-}$  and at pH lower than 3.5, the dominant species was  $VO_2H[EDTA]^{2-}$  [29]. For Ni-EDTA complex, at pH below 2.0, no Ni-EDTA complex formed. At pH between 2.0 and 6.0,  $NiH[EDTA]^-$  and at pH higher than 6.0,  $Ni[EDTA]^{2-}$  species was formed [30]. According to the negative charge of both V-EDTA and Ni-EDTA species and positive charge of NAC at the range of operational pH at RSM experiments, more numbers of the metal-ligand complex were adsorbed at the lower pH. The lower the pH, the greater the positive charge of the NAC surface. But, at the competitive experiments, differences between the charge of the V-EDTA and Ni-EDTA species made a difference, and selective adsorption occurred.

### 3.6. Adsorption isotherms

Fig. 3 shows the V-EDTA and Ni-EDTA experimental isotherms at three temperatures. As it is obvious, the amount of metal-ligand adsorption in both systems is decreased by temperature increase. So, it may be concluded the metal-ligand adsorption onto NAC is exothermic.

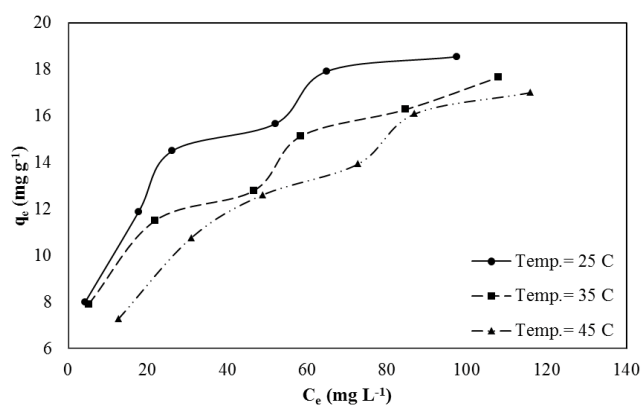
Four common isotherm models including Langmuir, Freundlich, Temkin, and Dubinin–Radushkevich, were studied for the equilibrium data. The Langmuir equation is shown at Eq. (10). Two consumptions were used to define this model, monolayer adsorption, and equal energy of all active sites [49]. By using the Langmuir constant ( $K_L$ ), a dimensionless constant of separation factor,  $R_L$ , was defined. The relation between  $R_L$  and  $K_L$  constants is illustrated at Eq. (11). The adsorption process is favorable if  $0 < R_L < 1$ . In the case of  $R_L > 1$ , the adsorption process is not favorable. Also,  $R_L = 1$  and  $R_L = 0$  indicate linear and irreversible adsorption process, respectively [50].

$$\frac{1}{q_e} = \frac{1}{q_{\max} K_L} \times \frac{1}{C_e} + \frac{1}{q_{\max}} \quad (10)$$

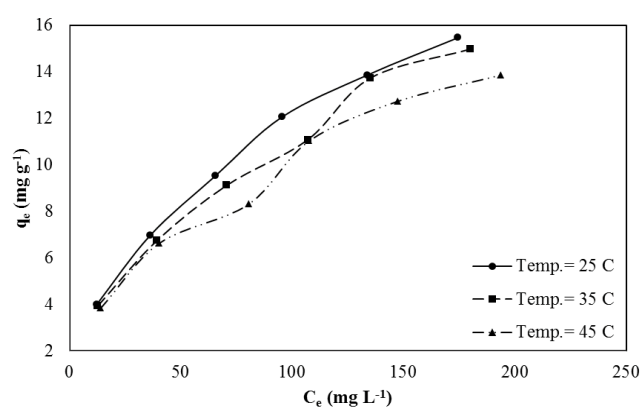
$$R_L = \frac{1}{1 + K_L C_{i,M}} \quad (11)$$

The parameter description of each isotherm model is reported in the nomenclature table.

Unlike the Langmuir isotherm, Freundlich isotherm could describe multilayer adsorption on heterogeneous



(a)



(b)

Fig. 3. Adsorption isotherms for (a) V-EDTA and (b) Ni-EDTA systems.

surfaces [51]. Moreover, it is assumed that active sites of the adsorbent have unequal energies, and stronger active sites are occupied first [52]. The Freundlich isotherm is shown at Eq. (12).

$$\log q_e = \frac{1}{n} \log C_e + \log K_F \quad (12)$$

At Temkin isotherm (Eq. (13)), the heat of adsorption for all adsorbate molecules in a layer follows from the linear decreasing form at the average concentration of the adsorbate [53].

$$q_e = B \ln K_T + B \ln C_e \quad (13)$$

To investigate the nature of the adsorption process (physical or chemical nature), Dubinin–Radushkevich isotherm was used (Eqs. (14) and (15)). The parameter  $E$  ( $J \text{ mol}^{-1}$ ), which demonstrates the free energy required for adsorption of one mole of adsorbate from bulk of the solution to the adsorbent surface, is used to find the adsorption nature. The relation between the parameter  $E$  and Dubinin–Radushkevich isotherm is as Eq. (16). The adsorption process has physical nature if the value of  $E$  is less than  $8 \text{ kJ mol}^{-1}$ . However, for the values between 8 and

16 kJ mol<sup>-1</sup>, it could be claimed that the process has chemical nature and controlled by electrostatic forces [54].

$$\ln q_e = \ln q_m - \beta \varepsilon^2 \quad (14)$$

$$\varepsilon = RT \ln \left( 1 + \frac{1}{C_e} \right) \quad (15)$$

$$E = \frac{1}{(2\beta)^{0.5}} \quad (16)$$

The parameters and constants of the four mentioned isotherm models are listed in Table 8. By investigating the  $R^2$  values, it was found that Freundlich and Dubinin–Radushkevich isotherms were the best models at all temperatures for both systems. The Langmuir isotherm predicted the  $q_{\max}$  to 17.67 mg g<sup>-1</sup> vanadium and 16.41 mg g<sup>-1</sup> nickel for V-EDTA and Ni-EDTA systems at 25°C, respectively. Also, by considering the  $K_L$  parameter and calculating the  $R_L$  values, it could be concluded that both metal-ligand

adsorptions were favorable. But, the  $R_L$  values for both systems were close to zero, which could be claimed the irreversibility. The values of the parameter  $n$  at Freundlich model proved favorability of the adsorption process. Similarly, this favorability was derived from the Langmuir model.

By analyzing the Temkin model, it was found that there is a proper fitting between the model behavior and experimental data. So, it seems that the heat of the adsorption processes followed a linear form. According to the Dubinin–Radushkevich isotherm and  $\beta$  parameter, the magnitude of the parameter  $E$  was calculated for both systems. According to these calculated values, the adsorption of V-EDTA and Ni-EDTA onto NAC had chemical nature, and the process was controlled by electrostatic attraction due to the charges of each component.

### 3.7. Thermodynamic parameters

The thermodynamic parameters, including change in free energy ( $\Delta G^\circ$ ), change in enthalpy ( $\Delta H^\circ$ ), and change in entropy ( $\Delta S^\circ$ ) were calculated by using the Langmuir

Table 8  
Parameters and constants of the isotherm models for both systems

Model	Parameter		Temperature (K)		
			298	308	318
Langmuir [52]	$K_L$	V-EDTA	9,701.220	9,317.603	2,545.879
		Ni-EDTA	1,308.213	1,348.944	1,279.935
	$q_{\max}$	V-EDTA	17.67	16.07	18.56
		Ni-EDTA	16.41	15.24	14.44
	$R_L$	V-EDTA	0.016–0.050	0.017–0.052	0.059–0.167
		Ni-EDTA	0.111–0.428	0.108–0.420	0.113–0.433
	$R^2$	V-EDTA	0.95	0.92	0.98
		Ni-EDTA	0.98	0.97	0.97
	$n$	V-EDTA	3.648	3.860	2.615
		Ni-EDTA	1.932	1.952	2.016
Freundlich [53]	$K_F$	V-EDTA	5.499	5.124	2.815
		Ni-EDTA	1.097	1.049	1.033
	$R^2$	V-EDTA	0.98	0.98	0.99
		Ni-EDTA	1.00	1.00	0.99
	$K_T$	V-EDTA	2.236	2.117	0.391
		Ni-EDTA	0.169	0.160	0.159
Temkin [54]	$B$	V-EDTA	3.446	3.097	4.383
		Ni-EDTA	4.355	4.186	3.854
	$R^2$	V-EDTA	0.97	0.95	0.98
		Ni-EDTA	0.97	0.94	0.95
	$\beta$	V-EDTA	$2.844 \times 10^{-9}$	$2.545 \times 10^{-9}$	$3.794 \times 10^{-9}$
		Ni-EDTA	$5.991 \times 10^{-9}$	$5.564 \times 10^{-9}$	$5.122 \times 10^{-9}$
Dubinin–Radushkevich [55]	$q_m$	V-EDTA	$7.344 \times 10^{-4}$	$6.245 \times 10^{-4}$	$8.945 \times 10^{-4}$
		Ni-EDTA	$9.870 \times 10^{-4}$	$9.125 \times 10^{-4}$	$8.146 \times 10^{-4}$
	$E$	V-EDTA	13.260	14.018	11.479
		Ni-EDTA	9.136	9.479	9.881
	$R^2$	V-EDTA	0.98	0.97	0.99
		Ni-EDTA	1.00	0.99	0.98

constant,  $K_L$ . By considering Eqs. (17)–(19), these thermodynamic parameters were calculated [6]. The plot of Eq. (19) for both V-EDTA and Ni-EDTA systems is illustrated in Fig. 4.

$$\ln(K_L) = -\frac{\Delta H^\circ}{RT} + \frac{\Delta S^\circ}{R} \quad (17)$$

$$\Delta G^\circ = -RT \ln(K_L) \quad (18)$$

$$T\Delta S^\circ = \Delta H^\circ - \Delta G^\circ \quad (19)$$

The thermodynamic parameters for both systems are reported in Table 9. According to this table, the negative values of  $\Delta G^\circ$  represent spontaneous adsorption for both V-EDTA and Ni-EDTA complexes. The adsorption of Ni-EDTA complex onto NAC was less exothermic than the V-EDTA adsorption. For this reason, the temperature had less effect on the Ni-EDTA isotherms (Fig. 3). The values of  $\Delta H^\circ$  confirmed this result. The negative and positive values of  $\Delta S^\circ$  represent decreasing and increasing of irregularities at the intersection of the adsorbent and solution at each system.

### 3.8. Adsorption kinetics

The kinetic tests were performed to determine the rate-controlling mechanism. At the mass transfer process, two mechanisms involved that are external diffusion (controlled by film resistance) and internal diffusion (controlled by intra-particle resistance) [6]. The effect of contact time for both V-EDTA and Ni-EDTA adsorptions onto NAC is shown in Fig. 5. The difference between the final  $q_t$  of these two systems is due to the differences in their operational parameters. The operational parameters at V-EDTA system are as follows:

- Initial vanadium concentration = 200 mg L<sup>-1</sup>, L/M ratio = 3, initial pH of the solutions = 2.0, and adsorbent dosage = 12 g L<sup>-1</sup>.

At earlier times of the process, the adsorption rate was high because of the high driving force at the first minutes of the process. Unlike conventional adsorption processes, this process is not merely incremental. Irregular increase and decrease, especially in the Ni-EDTA system are seen in the amount of  $q$ . This is probably due to the changes in the adsorbent and adsorbate charge during the process. According to section 3.1 (Characteristics of adsorbent),

during the process, OH<sup>-</sup> is released into the solution and leads to increase the solution pH. By increasing the pH of the solution, according to the adsorbent pH<sub>pzc</sub> (=8.3), electrostatic attraction between adsorbate and adsorbent becomes weak, and as a result, desorption occurs. After desorption, the adsorbate concentration increases in the solution and leads to increase in adsorption driving force; then adsorption process becomes dominant again. The continuous adsorption and desorption processes are the cause of fluctuations in the figure.

Four common kinetic models were used to investigate the adsorption kinetics of V-EDTA and Ni-EDTA. These models are pseudo-first-order, pseudo-second-order, intra-particle diffusion, and Boyd. The equations of these models are written in Table 10, including their parameters calculated by fitting them to the experimental data.

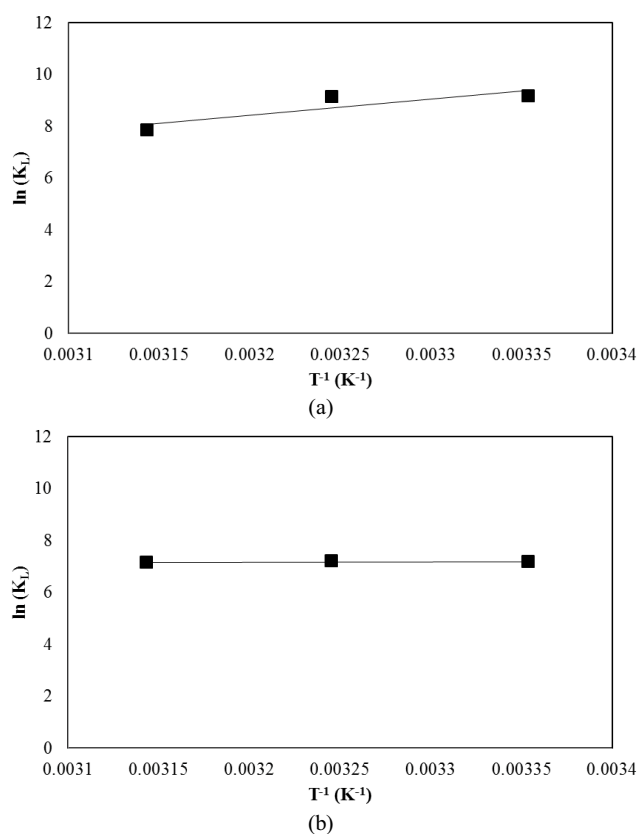


Fig. 4. Plot of  $\ln(K_L)$  vs.  $T^{-1}$  for (a) V-EDTA and (b) Ni-EDTA systems.

Table 9  
Thermodynamic parameters of V-EDTA and Ni-EDTA adsorptions

Temperature (K)	$\Delta G^\circ$ (kJ mol <sup>-1</sup> )		$\Delta H^\circ$ (kJ mol <sup>-1</sup> )		$T\Delta S^\circ$ (kJ mol <sup>-1</sup> )		$\Delta S^\circ$ (kJ mol <sup>-1</sup> K <sup>-1</sup> )	
	V-EDTA	Ni-EDTA	V-EDTA	Ni-EDTA	V-EDTA	Ni-EDTA	V-EDTA	Ni-EDTA
298	-22.756	-17.789			-29.440	16.963		
308	-23.415	-18.464	-52.196	-0.826	-28.781	17.638	-0.097	0.057
318	-20.743	-18.925			-31.435	18.099		

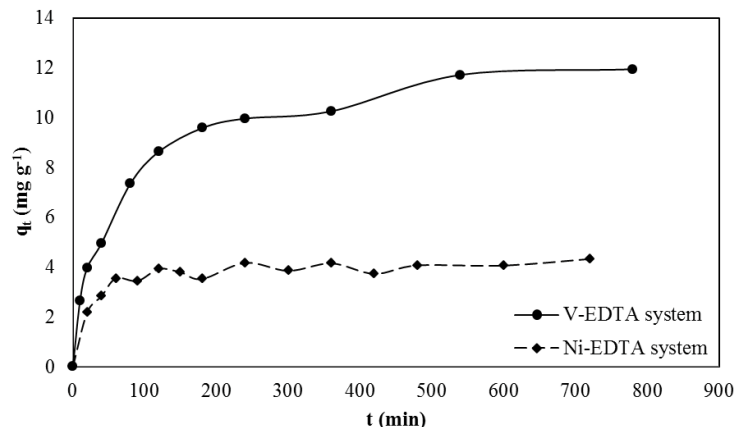


Fig. 5. Effect of contact time on metal-ligand adsorption.

According to Table 10 data and specifically the  $R^2$  values, it is evident that pseudo-second-order was the best model that can describe the experimental data for both V-EDTA and Ni-EDTA adsorptions onto NAC. The relative errors between experimental  $q_e$  and predicted  $q_e$  by this model are 0.46% and 1.15% for V-EDTA and Ni-EDTA, respectively. By considering the basis of the pseudo-second-order kinetic model is derived from a chemical reaction concept [58] and Dubinin–Radushkevich isotherm, which described the equilibrium data well, chemical nature (electrostatic attraction) of the V-EDTA and Ni-EDTA adsorption onto NAC is approved.

By analyzing the intra-particle diffusion model, the intra-particle diffusion mechanism was not rate controlling for the adsorption process in both systems. Hence in this model, the values of  $R^2$  at both systems are relatively low

and indicate a lack of fitness between the model behavior and experimental data. Also, the parameter  $C$  (intercept) indicates the model did not pass through the origin. To validate the result obtained from the intra-particle diffusion model, the Boyd model was analyzed. According to the low  $R^2$  values that indicate non-linearity and existence of intercepts in Boyd model, it could be concluded that the film diffusion mechanism controls the rate of mass transfer at both V-EDTA and Ni-EDTA adsorption processes.

### 3.9. Competitive adsorption

After investigating the adsorption of V-EDTA and Ni-EDTA individually on NAC, competitive experiments were done at three conditions:

Table 10  
Equations and constants of kinetic models for metal-ligand adsorption

Kinetic model	Equation	Parameter	Value	
			V-EDTA	Ni-EDTA
Experimental $q_e$ (calculated in kinetic investigations)			13.03	4.33
Pseudo-first-order [55]	$\ln(q_e - q_t) = \ln q_e - k_1 t$	$k_1$	0.0016	0.0029
		$q_e$	6.06	1.04
		$R^2$	0.76	0.47
Pseudo-second-order [56]	$\frac{t}{q_t} = \frac{1}{k_2 q_e^2} + \frac{1}{q_e} t$	$k_2$	0.0012	0.0107
		$q_e$	12.97	4.28
		$R^2$	1.00	0.99
Intra-particle diffusion [57]	$q_t = k_{\text{dif}} t^{0.5} + C$	$k_{\text{dif}}$	0.2260	0.0656
		$C$	4.7634	2.7025
		$R^2$	0.78	0.62
		$-0.4977 - \ln(1 - F) = B_i$	$B$	0.0016
Boyd [6]	$F = \frac{q_t}{q_e}$ $B = \frac{\pi^2 D_e}{r^2}$	Intercept	0.2671	0.9313
		$R^2$	0.76	0.47

- Condition 1:  $C_{i,V} = 120 \text{ mg L}^{-1}$ ,  $C_{i,Ni} = 40 \text{ mg L}^{-1}$ ,  $\text{pH}_i = 3.0$ , and  $C_{\text{Ads}} = 12 \text{ g L}^{-1}$ .
- Condition 2:  $C_{i,V} = 40 \text{ mg L}^{-1}$ ,  $C_{i,Ni} = 120 \text{ mg L}^{-1}$ ,  $\text{pH}_i = 3.0$ , and  $C_{\text{Ads}} = 12 \text{ g L}^{-1}$ .
- Condition 3:  $C_{i,V} = 120 \text{ mg L}^{-1}$ ,  $C_{i,Ni} = 120 \text{ mg L}^{-1}$ ,  $\text{pH}_i = 3.0$ , and  $C_{\text{Ads}} = 12 \text{ g L}^{-1}$ .

To evaluate NAC performance and its selectivity in adsorption of metal-ligand complexes, both adsorption percentage and  $q_M$  were reported in Figs. 6 and 7, respectively.

In Fig. 6a, the adsorption percentages after 7 h for V-EDTA and Ni-EDTA systems were 50.52% and 12.17%, respectively. Also, by considering Fig. 7a, the ratio of  $q_V/q_{Ni}$  was 11.84 at the end of the adsorption process. This ratio is perfect for a selective process. Two factors were involved to obtain this proper ratio. The first factor was higher V-EDTA complex driving force due to its higher initial concentration, and the second factor was NAC selectivity on V-EDTA complex, which is more important.

According to Fig. 6b, after 7 h, 73.92% of V-EDTA complex was adsorbed. While in the same period, just 26.59% of Ni-EDTA complex was adsorbed. In this condition, although the adsorption driving force for Ni-EDTA complex was higher than V-EDTA, higher amounts of V-EDTA complex were adsorbed due to NAC selectivity to V-EDTA complex. But, the higher initial concentration of Ni-EDTA complex influenced adsorbent capacities that is visible in Fig. 7b. It caused an increase in Ni-EDTA adsorbent capacity compared to condition 1. The  $q_M$  at the end of the process for V-EDTA and Ni-EDTA systems were 2.86 and 2.94  $\text{mg L}^{-1}$ , respectively.

The results related to equal initial concentrations (condition 3) are illustrated in Figs. 6c and 7c. After 7h, 54.30% of V-EDTA and 19.97% of Ni-EDTA were adsorbed. Due to the equal initial concentration of both complexes, the selectivity of NAC on V-EDTA complex was clear. Also, the end of the process  $q_V/q_{Ni}$  was 2.68, which is a good value. According to the literature review, in most cases, which vanadium and nickel metals need to be separated from their resources, the amount of nickel is less than vanadium amounts [4,15,17,59]. It is equivalent to condition 1, and the results obtained from this condition indicate that the adsorbent (NAC) has very good selectivity.

To justify the selectivity of NAC on V-EDTA complex, two mechanisms were investigated. First, the tendency of NAC surface to make a chemical bond with metal-ligand complex and at the second step, diffuse of the metal-ligand complexes from the bulk of the solution to inner layers of the adsorbent were studied. To do this, the results of equilibrium and kinetic studies were used.

By studying the pseudo-second-order kinetic model and Dubinin–Radushkevich isotherm, it was found that the natures of the adsorption for both systems are chemical. Also, the  $E$  parameters at 25°C for V-EDTA and Ni-EDTA systems were 13.260 and 9.136  $\text{kJ mol}^{-1}$ , respectively. It was also mentioned that if the value of parameter  $E$  is smaller than 8  $\text{kJ mol}^{-1}$ , the nature of the adsorption is physical. It means as the amount of the parameter  $E$  decreases, the strength of the bond between the adsorbent surface and the components decreases too. So, the strength of the bond between Ni-EDTA complex and NAC surface was weak

in comparison to V-EDTA complex. Moreover, the calculated values of  $\Delta G^\circ$  at 25°C for V-EDTA and Ni-EDTA systems ( $-22.756$  and  $-17.789 \text{ kJ mol}^{-1}$ ) indicate the more adsorption tendency for V-EDTA onto NAC surface.

The Boyd model was used to distinguish the mass transfer resistance between film diffusion and intra-particle diffusion. It was found that the film diffusion mechanism may be the rate-controlling step in both adsorption systems. In Boyd model, according to the  $R^2$  values, the non-linearity of experimental data in comparison to the model behavior at Ni-EDTA system was higher than V-EDTA system. Moreover, the intercept at Ni-EDTA system was more than the intercept at V-EDTA system. These two may indicate the more significant film diffusion resistance for Ni-EDTA complex.

At initial  $\text{pH} = 3.0$ , V-EDTA species is  $\text{VO}_2\text{H}[\text{EDTA}]^{2-}$  and Ni-EDTA species are  $\text{NiH}[\text{EDTA}]^-$  and  $\text{Ni}[\text{EDTA}]^{2-}$  [29,30]. Based on the obtained results, it could be concluded that chemical structure differences in V-EDTA and Ni-EDTA species, such as the existence of oxygen in V-EDTA species, made differences in the number of their adsorptions and more NAC tendency to adsorb V-EDTA complex.

### 3.10. Kinetics in competitive adsorption

The experimental data of competitive adsorption were investigated with the following kinetic models at each condition to obtain a modified kinetic model that can describe the whole process:

- Pseudo-first-order, pseudo-second-order, intra-particle, and Boyd.

The results of this investigation are listed in Table 11. According to this table, the pseudo-second-order kinetic model could describe the adsorption data well. So, this model was chosen, and its parameters including  $q_e$  and  $k_2$  were found in terms of initial concentrations ratio of metals ( $C_{i,V}/C_{i,Ni}$ ).

To find the relationship between the model parameters ( $q_e$  and  $k_2$ ) and the initial concentration ratio of metals, the same pseudo-second-order model was used for the first time in this paper. As time passes, concentrations of the components vary, too. So in the pseudo-second-order model, the parameter that indicates the time ( $t$ ) was substituted with the concentration indicator term ( $C_{i,V}/C_{i,Ni}$ ). The parameter  $q_i$  in the model was also substituted with  $q_e$  and  $k_2$ , which have the same concept according to their units.

The modified pseudo-second-order kinetic model that is describing the competitive adsorption of V-EDTA component is shown in Eqs. (20)–(22). The regression coefficient of both Eqs. (21) and (22) was 0.98.

$$\frac{t}{q_{i,V}} = \frac{1}{k_{2,V}q_{e,V}^2} + \frac{1}{q_{e,V}}t \quad (20)$$

$$\left( \frac{C_{i,V}}{C_{i,Ni}} \right) \frac{1}{k_{2,V}} = -32.1009 + 295.5460 \frac{C_{i,V}}{C_{i,Ni}} \quad (21)$$

$$\left(\frac{C_{i,V}}{C_{i,Ni}}\right) = 0.0348 + 0.1572 \frac{C_{i,V}}{C_{i,Ni}} \quad (22)$$

where  $q_{i,V}$  and  $q_{e,V}$  are the amounts of vanadium adsorbed per unit weight of NAC ( $\text{mg g}^{-1}$ ) at time  $t$  (min) and equilibrium, respectively.  $k_{2,V}$  is the rate constant of pseudo-second-order

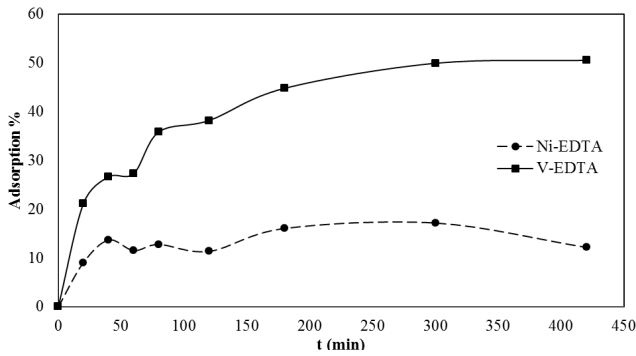
kinetic model ( $\text{g mg}^{-1} \text{min}^{-1}$ ) modified for describing V-EDTA competitive adsorption.

Similarly, the modified pseudo-second-order kinetic model for competitive adsorption of Ni-EDTA component onto NAC is illustrated in Eqs. (23)–(25). For both Eqs. (24) and (25), the regression coefficient was found 0.98.

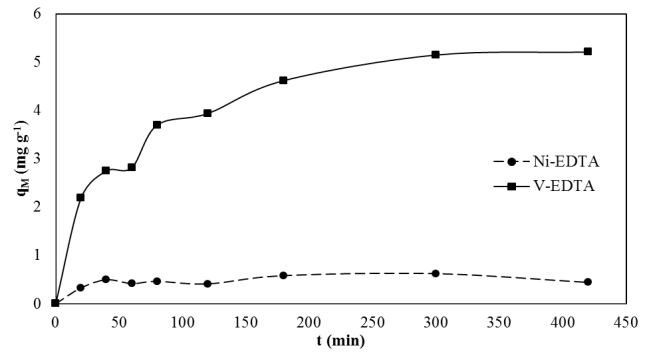
$$\frac{t}{q_{i,Ni}} = \frac{1}{k_{2,Ni}q_{e,Ni}^2} + \frac{1}{q_{e,Ni}}t \quad (23)$$

Table 11  
Parameters of kinetic models for metal-ligand adsorption in competitive experiments

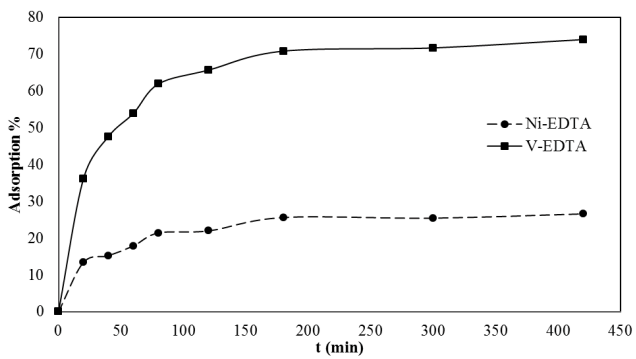
$C_{i,V}/C_{i,Ni}$	Kinetic model	Parameter	Value		
			V-EDTA component	Ni-EDTA component	
1/3	Experimental, $q_e$ (after 7 h)		2.86	2.94	
	Pseudo-first-order	$k_1$	0.0115	0.0108	
		$q_e$	1.63	1.81	
		$R^2$	0.90	0.85	
	Pseudo-second-order	$k_2$	0.0141	0.0109	
		$q_e$	3.02	3.13	
		$R^2$	1.00	1.00	
	Intra-particle diffusion	$k_{\text{dif}}$	0.1257	0.1309	
		$C$	0.8183	0.7526	
		$R^2$	0.77	0.81	
		$B$	0.01147	0.0108	
		$R^2$	0.0627	-0.0150	
	1	Experimental, $q_e$ (after 7 h)		5.63	2.10
		Pseudo-first-order	$k_1$	0.0084	0.0087
			$q_e$	4.26	1.46
$R^2$			0.97	0.72	
Pseudo-second-order		$k_2$	0.0031	0.0195	
		$q_e$	6.21	1.92	
		$R^2$	1.00	0.93	
Intra-particle diffusion		$k_{\text{dif}}$	0.2595	0.0943	
		$C$	0.9250	0.4418	
		$R^2$	0.92	0.84	
		$B$	0.0084	0.0087	
		$R^2$	-0.2192	-0.1335	
3		Experimental $q_e$ (after 7 h)		5.21	0.44
		Pseudo-first-order	$k_1$	0.0138	(Not applicable)
			$q_e$	5.00	(Not applicable)
	$R^2$		0.97	(Not applicable)	
	Pseudo-second-order	$k_2$	0.0036	0.0355	
		$q_e$	5.83	0.69	
		$R^2$	1.00	0.96	
	Intra-particle diffusion	$k_{\text{dif}}$	0.2467	0.0203	
		$C$	0.9153	0.2156	
		$R^2$	0.90	0.52	
		$B$	0.0138	(Not applicable)	
		$R^2$	-0.4559	(Not applicable)	
	Boyd	Intercept	-0.4559	(Not applicable)	
		$R^2$	0.97	(Not applicable)	



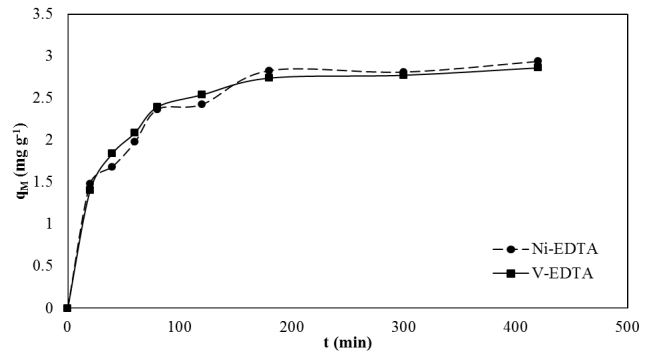
(a)



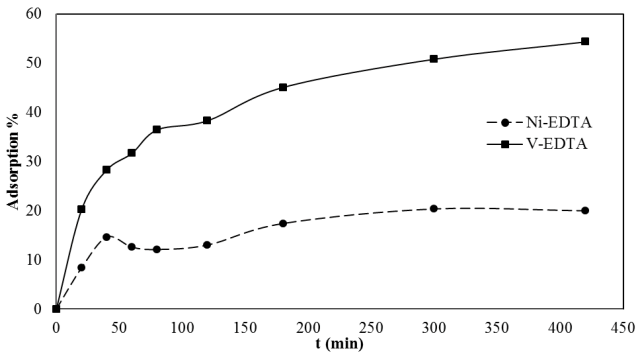
(a)



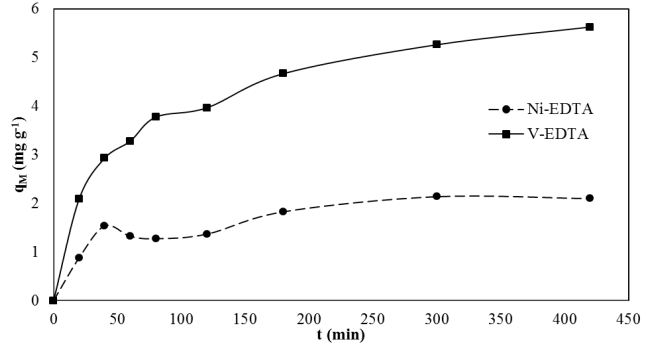
(b)



(b)



(c)



(c)

Fig. 6. Adsorption percentage of metal-ligand vs. time (min) in competitive experiments at (a) condition 1, (b) condition 2, and (c) condition 3.

Fig. 7.  $q_M$  of metal-ligand systems vs. time (min) in competitive experiments at (a) condition 1, (b) condition 2, and (c) condition 3.

$$\left(\frac{C_{i,V}}{C_{i,Ni}}\right) = 27.4961 + 19.3504 \frac{C_{i,V}}{C_{i,Ni}} \quad (24)$$

$$\left(\frac{C_{i,V}}{C_{i,Ni}}\right) = -0.7494 + 1.6690 \frac{C_{i,V}}{C_{i,Ni}} \quad (25)$$

where  $q_{i,Ni}$ ,  $q_{e,Ni}$  and  $k_{2,Ni}$  are the same as the previous model but for Ni-EDTA competitive adsorption. It should be noted

that these modified kinetic models are valid in the concentration range of 40–120 mg L<sup>-1</sup> for each metal and in the period of at 0–7 h.

### 3.11. Free EDTA and Na adsorptions in competitive experiments

As mentioned earlier, the dominant species of free EDTA at competitive experiments (pH<sub>i</sub> = 3.0) are H<sub>3</sub>[EDTA]<sup>-</sup> and H<sub>2</sub>[EDTA]<sup>2-</sup> [48]. Due to the negative charge of these species, adsorptions of them occurred. The adsorption percentage and  $q_{EDTA}$  vs. time are illustrated in Fig. 8.

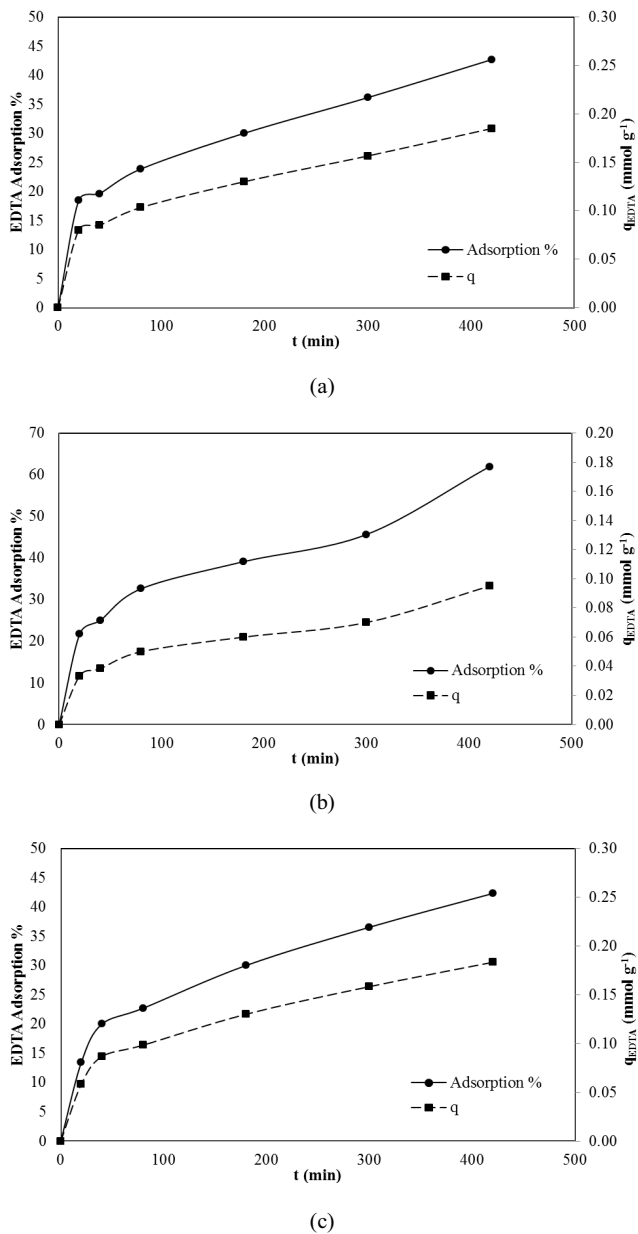


Fig. 8. Adsorption percentage and  $q_{\text{EDTA}}$  vs. time (min) in competitive experiments at (a) condition 1, (b) condition 2, and (c) condition 3.

The initial concentration of EDTA was measured 5.20 mM at both conditions 1 and 3. Because in these conditions, the initial concentration of vanadium is equal to 120 mg  $\text{L}^{-1}$  and the molar ratio of EDTA to vanadium is constant and equal to 3. In condition 2, the initial concentration of EDTA was measured 1.84 mM.

According to Fig. 8, after 7 h, the EDTA adsorption percentage in condition 2 becomes 61.96% and 42.69% and 42.31%, respectively, in conditions 1 and 3. In condition 2, due to the lower initial concentration of EDTA, the value of adsorption percentage has become higher than the values in conditions 1 and 3. Since the initial concentration of EDTA is higher in conditions 1 and 3, the  $q_{\text{EDTA}}$  in these conditions

was found higher than condition 2. After 7 h, the  $q_{\text{EDTA}}$  in conditions 1, 2, and 3 were 0.185, 0.095, and 0.183 mmol  $\text{g}^{-1}$ , respectively.

Because the sodium salt of EDTA was used to prepare the solutions,  $\text{Na}^+$  cation was present in all experiments. According to the EDTA salt ( $\text{Na}_2\text{EDTA}\cdot 2\text{H}_2\text{O}$ ), the molar ratio of Na to total EDTA (including in complex and free EDTA) was 2. It is predicted that  $\text{Na}^+$  has low adsorption onto NAC due to its positive charge in low concentrations. But in competitive experiments, the Na concentrations were relatively high, which were 500, 356, and 631 mg  $\text{L}^{-1}$  at conditions 1, 2, and 3, respectively. These high concentrations result in having a high driving force for Na adsorption.

In Fig. 9, the adsorption percentage and  $q_{\text{Na}}$  are shown. According to the results, in condition 1 where the nickel concentration was low, the adsorption of Na was high in comparison to the other conditions. The reason may be the existence of nitrate in the solution that came from nickel salt ( $\text{NiN}_2\text{O}_6\cdot 6\text{H}_2\text{O}$ ). The  $[\text{NO}_3]^{2-}$  component that has a negative charge, is adsorbed onto NAC and block the active sites. So, in conditions 2 and 3 where the nickel concentration is higher than condition 1, the nitrate may block some of NAC active sites and as a result, the lower amounts of Na were adsorbed.

The adsorption percentage and  $q_{\text{Na}}$  in condition 1 after 7 h were 17.07% and 7.13 mg  $\text{g}^{-1}$ , respectively. Similarly in condition 2, at the end of the process, the adsorption percentage and  $q_{\text{Na}}$  were 6.83% and 2.27 mg  $\text{g}^{-1}$ , respectively. In condition 3, where both initial concentrations of metals were equal to 120 mg  $\text{L}^{-1}$  and according to the maximum existence of nitrate and V-EDTA component, the value of Na adsorption was lower than the values at other conditions. The values of 2.95% and 1.55 mg  $\text{g}^{-1}$  were the adsorption percentage and  $q_{\text{Na}}$  at condition 3 after 7 h, respectively.

#### 4. Conclusion

At optimum operational conditions in individual investigations, the  $q_{\text{max}}$  at V-EDTA system was predicted 15.39 mg  $\text{g}^{-1}$  V with a relative error of 8.67% and at Ni-EDTA system was predicted 15.82 mg  $\text{g}^{-1}$  Ni with a relative error of 8.73% by the models. The optimum operational conditions at V-EDTA system were  $C_{i,V} = 200$  mg  $\text{L}^{-1}$ ,  $L/M = 1$ ,  $\text{pH}_i = 2.0$ , and  $C_{\text{Ads}} = 2$  g  $\text{L}^{-1}$ , and at Ni-EDTA system were  $C_{i,Ni} = 200$  mg  $\text{L}^{-1}$ ,  $L/M = 1$ ,  $\text{pH}_i = 3.0$ , and  $C_{\text{Ads}} = 2$  g  $\text{L}^{-1}$ , and contact time at both systems was 4 h. The statistical data and diagnostic plots showed the significance of the models. The pseudo-second-order kinetic model described the experimental kinetic data well for both systems. The Freundlich and Dubinin–Radushkevich isotherms were fitted to the equilibrium data at both V-EDTA and Ni-EDTA systems. According to the kinetics and equilibrium investigations, it was found that both adsorptions of V-EDTA and Ni-EDTA complexes onto NAC had the chemical nature (electrostatic attraction) and controlled by film diffusion. Likewise, they were exothermic, spontaneous, and feasible. Competitive experiments were done kinetically at three operational conditions based on the optimum results derived from the RSM. At one of these conditions that were closer to industrial cases, the ratio of complexed vanadium to nickel adsorbed ( $q_{\text{V}}/q_{\text{Ni}}$ ) was found 11.84 that is acceptable for a

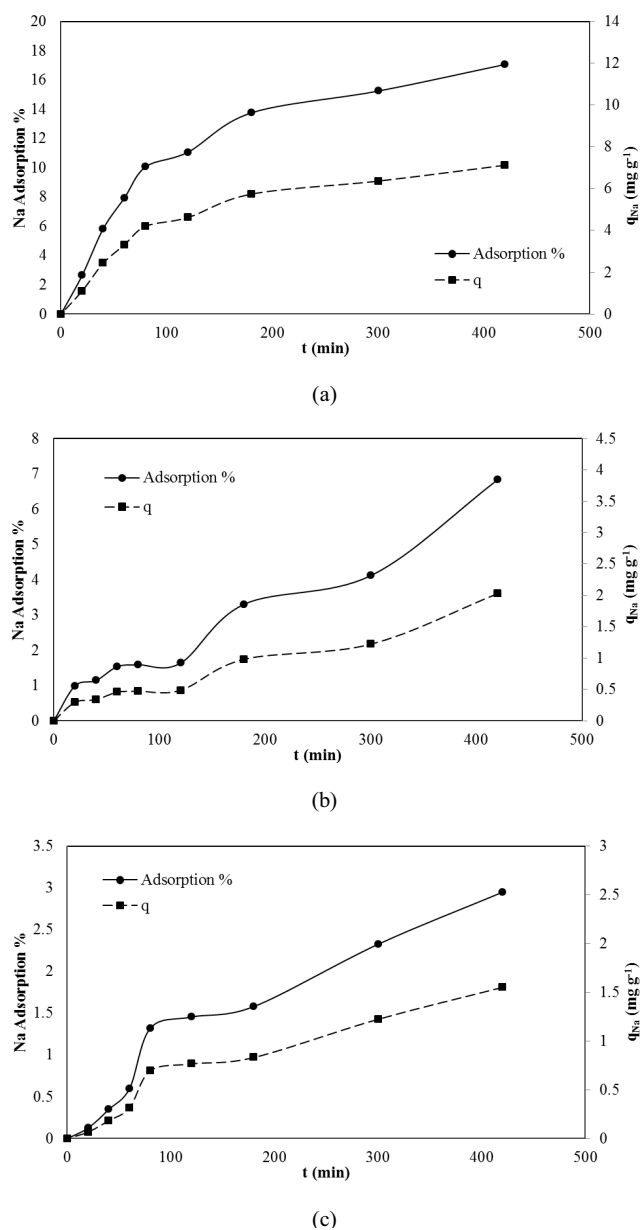


Fig. 9. Adsorption percentage and  $q_{\text{Na}}$  vs. time (min) in competitive experiments at (a) condition 1, (b) condition 2, and (c) condition 3.

selective adsorption process. Moreover, a modified pseudo-second-order kinetic model was introduced for the first time to describe the whole competitive adsorption process well.

### Funding

This research did not receive any specific grant from funding agencies in the public, commercial, or not-for-profit sectors.

### Symbols

$B$  — Constant of Temkin isotherm that is related to the heat of adsorption,  $\text{J mol}^{-1}$

- $C$  — Intercept of intra-particle diffusion kinetic model,  $\text{mg g}^{-1}$
- $C_e$  — Concentration of vanadium or nickel at equilibrium,  $\text{mg L}^{-1}$  or  $\text{mol L}^{-1}$
- $D_e$  — Effective diffusion coefficient of Boyd kinetic model,  $\text{m}^2 \text{s}^{-1}$
- $k_1$  — Rate constant of pseudo-first-order kinetic model,  $\text{min}^{-1}$
- $k_2$  — Rate constant of pseudo-second-order kinetic model,  $\text{g mg}^{-1} \text{min}^{-1}$
- $k_{\text{dif}}$  — Rate constant of intra-particle diffusion kinetic model,  $\text{mg g}^{-1} \text{min}^{-0.5}$
- $K_F$  — Constant of Freundlich isotherm that is related to the adsorption capacity of the adsorbent,  $\text{mg}^{1-(1/n)} \text{L}^{1/n} \text{g}^{-1}$
- $K_L$  — Constant of Langmuir isotherm that is related to the energy of adsorption,  $\text{L mol}^{-1}$
- $K_T$  — Equilibrium binding constant that is related to the maximum binding energy,  $\text{L mg}^{-1}$
- $n$  — Exponent of Freundlich isotherm that is related to the adsorption intensity
- $q_e$  — Amount of vanadium or nickel adsorbed per unit weight of the adsorbent at equilibrium,  $\text{mg g}^{-1}$
- $q_m$  — Theoretical saturation capacity,  $\text{mol g}^{-1}$
- $q_{\text{max}}$  — Maximum adsorption capacity of the adsorbent,  $\text{mg g}^{-1}$
- $q_t$  — Amount of vanadium or nickel adsorbed per unit weight of the adsorbent at time  $t$ ,  $\text{mg g}^{-1}$
- $r$  — Radius of the adsorbent particles,  $\text{m}$
- $R$  — Universal gas constant,  $8.3145 \text{ J mol}^{-1} \text{ K}^{-1}$
- $t$  — Time,  $\text{min}$
- $T$  — Temperature,  $\text{K}$
- $B$  — Constant term of Dubinin–Radushkevich isotherm that is related to the mean free energy of adsorption per mole of the adsorbate,  $\text{mol}^2 \text{ J}^{-2}$
- $\varepsilon$  — Polanyi potential term of Dubinin–Radushkevich isotherm that is related to the equilibrium concentration,  $\text{J mol}^{-1}$

### References

- [1] D.G. Barceloux, D. Barceloux, Vanadium, *J. Toxicol. Clin. Toxicol.*, 37 (1999) 265–278.
- [2] R.S. Drago, E.I. Baucom, Stabilization of high oxidation states of nickel with pyridine oxime ligands, *Inorg. Chem.*, 11 (1972) 2064–2069.
- [3] L. Sacconi, C. Ghilardi, C. Mealli, F. Zanobini, Synthesis, properties, and structural characterization of complexes of cobalt and nickel in low oxidation states with the tripod ligand tris (2-diphenylphosphinoethyl) amine, *Inorg. Chem.*, 14 (1975) 1380–1386.
- [4] M.F. Ali, S. Abbas, A review of methods for the demetallization of residual fuel oils, *Fuel Process. Technol.*, 87 (2006) 573–584.
- [5] T. Sakai, H. Miyamura, N. Kuriyama, I. Uehara, M. Muta, A. Takagi, U. Kajiyama, K. Kinoshita, F. Isogai, Nickel-metal hydride battery for electric vehicles, *J. Alloys Compd.*, 192 (1993) 158–160.
- [6] H. Sharififard, M. Soleimani, Performance comparison of activated carbon and ferric oxide-hydroxide-activated carbon nanocomposite as vanadium(V) ion adsorbents, *RSC Adv.*, 5 (2015) 80650–80660.
- [7] C. Shen, W. Zhou, H. Yu, L. Du, Ni nanoparticles supported on carbon as efficient catalysts for steam reforming of toluene (model tar), *Chin. J. Chem. Eng.*, 26 (2018) 322–329.
- [8] A. Phasuk, S. Srisantitham, T. Tuntulani, W. Anutrasakda, Facile synthesis of magnetic hydroxyapatite-supported nickel

- oxide nanocomposite and its dye adsorption characteristics, *Adsorption*, 24 (2018) 157–167.
- [9] M. Saeed, S. Adeel, M. Ilyas, M.A. Shahzad, M. Usman, E.-u. Haq, M. Hamayun, Oxidative degradation of Methyl Orange catalyzed by lab prepared nickel hydroxide in aqueous medium, *Desal. Water Treat.*, 57 (2016) 12804–12813.
- [10] N. Larché, P. Boillot, P. Dezerville, E. Johansson, J. Lardon, D. Thierry, Crevice corrosion performance of high-alloy stainless steels and Ni-based alloy in desalination industry, *Desal. Water Treat.*, 55 (2015) 2491–2501.
- [11] E.M. Choi, M.K. Kim, E.T. Kang, K.B. Kang, D.S. Kim, Perfluorinated polymer for vanadium flow battery, *Desal. Water Treat.*, 51 (2013) 5172–5178.
- [12] I. Ghouma, M. Guiza, M. Jeguirim, A.A. Zorpas, L. Limousy, A. Ouederni, An optimization study of nickel catalyst supported on activated carbon for the 2-nitrophenol catalytic ozonation, *Desal. Water Treat.*, 112 (2018) 242–249.
- [13] Z. Zhao, M. Guo, M. Zhang, Extraction of molybdenum and vanadium from the spent diesel exhaust catalyst by ammonia leaching method, *J. Hazard. Mater.*, 286 (2015) 402–409.
- [14] L. Zeng, C.Y. Cheng, A literature review of the recovery of molybdenum and vanadium from spent hydrodesulphurisation catalysts: part II: separation and purification, *Hydrometallurgy*, 98 (2009) 10–20.
- [15] S. Goel, K. Pant, K. Nigam, Extraction of nickel from spent catalyst using fresh and recovered EDTA, *J. Hazard. Mater.*, 171 (2009) 253–261.
- [16] I.S. Pinto, H.M. Soares, Microwave-assisted selective leaching of nickel from spent hydrodesulphurization catalyst: a comparative study between sulphuric and organic acids, *Hydrometallurgy*, 140 (2013) 20–27.
- [17] M.A. Al-Ghouti, Y.S. Al-Degs, A. Ghrair, H. Khoury, M. Ziedan, Extraction and separation of vanadium and nickel from fly ash produced in heavy fuel power plants, *Chem. Eng. J.*, 173 (2011) 191–197.
- [18] A. Padilla-Rodríguez, J.A. Hernández-Viezas, J.R. Peralta-Videa, J.L. Gardea-Torresdey, O. Perales-Pérez, F.R. Román-Velázquez, Synthesis of protonated chitosan flakes for the removal of vanadium(III, IV and V) oxyanions from aqueous solutions, *Microchem. J.*, 118 (2015) 1–11.
- [19] M. Alibrahim, H. Shlewit, S. Alike, Solvent extraction of vanadium(IV) with di (2-ethylhexyl) phosphoric acid and tributyl phosphate, *Period. Polytech. Chem. Eng.*, 52 (2008) 29–33.
- [20] M. Nabavinia, M. Soleimani, A. Kargari, Vanadium recovery from oil refinery sludge using emulsion liquid membrane technique, *Int. J. Chem. Environ. Eng.*, 3 (2012) 149–152.
- [21] S. Ramírez, P. Schacht, R. Quintana-Solórzano, J. Aguilar, Leaching of heavy metals under ambient resembling conditions from hydrotreating spent catalysts, *Fuel*, 110 (2013) 286–292.
- [22] B. Nowack, J.M. VanBrienen, Chelating agents in the environment, *Biogeochem. Chelating Agents*, 910 (2005) 1–18.
- [23] M. Kavand, T. Kaghazchi, M. Soleimani, Optimization of parameters for competitive adsorption of heavy metal ions ( $Pb^{2+}$ ,  $Ni^{2+}$ ,  $Cd^{2+}$ ) onto activated carbon, *Korean J. Chem. Eng.*, 31 (2014) 692–700.
- [24] H. Sharififard, F. Zokaei Ashtiani, M. Soleimani, Adsorption of palladium and platinum from aqueous solutions by chitosan and activated carbon coated with chitosan, *Asia-Pac. J. Chem. Eng.*, 8 (2013) 384–395.
- [25] M. Barkat, D. Nibou, S. Chegrouche, A. Mellah, Kinetics and thermodynamics studies of chromium(VI) ions adsorption onto activated carbon from aqueous solutions, *Chem. Eng. Process. Process Intensif.*, 48 (2009) 38–47.
- [26] M. Poorbaba, M. Soleimani, Recovery of vanadium–EDTA complex from extraction leachate of vanadium secondary resources: optimization and experimental investigation, *Desal. Water Treat.*, 101 (2018) 268–282.
- [27] S. Brunauer, P.H. Emmett, E. Teller, Adsorption of gases in multimolecular layers, *J. Am. Chem. Soc.*, 60 (1938) 309–319.
- [28] S.A. Dastgheib, D.A. Rockstraw, A model for the adsorption of single metal ion solutes in aqueous solution onto activated carbon produced from pecan shells, *Carbon*, 40 (2002) 1843–1851.
- [29] A. Ringbom, S. Siitonen, B. Skrifvars, The ethylenediamine-tetraacetate complexes of vanadium(V), *Acta Chem. Scand.*, 11 (1957) 551–554.
- [30] D. Bhattacharyya, C.R. Cheng, Activated carbon adsorption of heavy metal chelates from single and multicomponent systems, *Environ. Prog.*, 6 (1987) 110–118.
- [31] H.-s. Zhu, X.-j. Yang, Y.-p. Mao, Y. Chen, X.-l. Long, W.-k. Yuan, Adsorption of EDTA on activated carbon from aqueous solutions, *J. Hazard. Mater.*, 185 (2011) 951–957.
- [32] M. Kavand, M. Soleimani, T. Kaghazchi, N. Asasian, Competitive separation of lead, cadmium, and nickel from aqueous solutions using activated carbon: response surface modeling, equilibrium, and thermodynamic studies, *Chem. Eng. Commun.*, 203 (2016) 123–135.
- [33] N. Mehrabi, M. Soleimani, M.M. Yeganeh, H. Sharififard, Parameter optimization for nitrate removal from water using activated carbon and composite of activated carbon and  $Fe_2O_3$  nanoparticles, *RSC Adv.*, 5 (2015) 51470–51482.
- [34] D.L. Pavia, G.M. Lampman, G.S. Kriz, J.A. Vyvyan, *Introduction to Spectroscopy*, Cengage Learning, California, 2009.
- [35] K.Y. Nandiwale, N.D. Galande, V.V. Bokade, Process optimization by response surface methodology for transesterification of renewable ethyl acetate to butyl acetate biofuel additive over borated USY zeolite, *RSC Adv.*, 5 (2015) 17109–17116.
- [36] M.R. Hormozi-Nezhad, M. Jalali-Heravi, H. Robotjazi, H. Ebrahimi-Najafabadi, Controlling aspect ratio of colloidal silver nanorods using response surface methodology, *Colloids Surf., A*, 393 (2012) 46–52.
- [37] T. Ölmez, The optimization of Cr(VI) reduction and removal by electrocoagulation using response surface methodology, *J. Hazard. Mater.*, 162 (2009) 1371–1378.
- [38] A. Nezamzadeh-Ejhieh, M. Kabiri-Samani, Effective removal of Ni(II) from aqueous solutions by modification of nano particles of clinoptilolite with dimethylglyoxime, *J. Hazard. Mater.*, 260 (2013) 339–349.
- [39] R. Kumar, M. Barakat, Y. Daza, H. Woodcock, J. Kuhn, EDTA functionalized silica for removal of Cu(II), Zn(II) and Ni(II) from aqueous solution, *J. Colloid Interface Sci.*, 408 (2013) 200–205.
- [40] E. Repo, T.A. Kurniawan, J.K. Warchol, M.E. Sillanpää, Removal of Co(II) and Ni(II) ions from contaminated water using silica gel functionalized with EDTA and/or DTPA as chelating agents, *J. Hazard. Mater.*, 171 (2009) 1071–1080.
- [41] S.Z. Mohammadi, H. Hamidian, Z. Moeinadini, High surface area-activated carbon from *Glycyrrhiza glabra* residue by  $ZnCl_2$  activation for removal of Pb(II) and Ni(II) from water samples, *J. Ind. Eng. Chem.*, 20 (2014) 4112–4118.
- [42] W.A. Carvalho, C. Vignado, J. Fontana, Ni(II) removal from aqueous effluents by silylated clays, *J. Hazard. Mater.*, 153 (2008) 1240–1247.
- [43] T. Anirudhan, P. Radhakrishnan, Adsorptive performance of an amine-functionalized poly(hydroxyethylmethacrylate)-grafted tamarind fruit shell for vanadium(V) removal from aqueous solutions, *Chem. Eng. J.*, 165 (2010) 142–150.
- [44] T. Wang, Z. Cheng, B. Wang, W. Ma, The influence of vanadate in calcined Mg/Al hydrotalcite synthesis on adsorption of vanadium(V) from aqueous solution, *Chem. Eng. J.*, 181 (2012) 182–188.
- [45] A. Bhatnagar, A.K. Minocha, D. Pudasainee, H.-K. Chung, S.-H. Kim, H.-S. Kim, G. Lee, B. Min, B.-H. Jeon, Vanadium removal from water by waste metal sludge and cement immobilization, *Chem. Eng. J.*, 144 (2008) 197–204.
- [46] C. Namasivayam, D. Sangeetha, Removal and recovery of vanadium(V) by adsorption onto  $ZnCl_2$  activated carbon: kinetics and isotherms, *Adsorption*, 12 (2006) 103–117.
- [47] A. Etaati, M. Soleimani, Optimizing of vanadium adsorption onto natural bentonite using response surface methodology, *Int. J. Chem. Environ. Eng.*, 6 (2015) 357–361.
- [48] K. Zohdy, Surface protection of carbon steel in acidic solution using ethylenediaminetetraacetic disodium salt, *Int. J. Electrochem. Sci.*, 10 (2015) 414–431.

- [49] I. Langmuir, The constitution and fundamental properties of solids and liquids. Part I. Solids, *J. Am. Chem. Soc.*, 38 (1916) 2221–2295.
- [50] K.R. Hall, L.C. Eagleton, A. Acrivos, T. Vermeulen, Pore-and solid-diffusion kinetics in fixed-bed adsorption under constant-pattern conditions, *Ind. Eng. Chem. Fundam.*, 5 (1966) 212–223.
- [51] A. Heidari, H. Younesi, Z. Mehraban, H. Heikkinen, Selective adsorption of Pb(II), Cd(II), and Ni(II) ions from aqueous solution using chitosan–MAA nanoparticles, *Int. J. Biol. Macromol.*, 61 (2013) 251–263.
- [52] I. Tan, A. Ahmad, B. Hameed, Adsorption isotherms, kinetics, thermodynamics and desorption studies of 2,4,6-trichlorophenol on oil palm empty fruit bunch-based activated carbon, *J. Hazard. Mater.*, 164 (2009) 473–482.
- [53] G.S. ElShafei, I. Nasr, A.S. Hassan, S. Mohammad, Kinetics and thermodynamics of adsorption of cadusafos on soils, *J. Hazard. Mater.*, 172 (2009) 1608–1616.
- [54] C. Wang, J. Ni, J. Zhou, J. Wen, X. Lü, Strategically designed porous polysilicate acid/graphene composites with wide pore size for methylene blue removal, *RSC Adv.*, 3 (2013) 23139–23145.
- [55] H. Yuh-Shan, Citation review of Lagergren kinetic rate equation on adsorption reactions, *Scientometrics*, 59 (2004) 171–177.
- [56] Y.-S. Ho, Second-order kinetic model for the sorption of cadmium onto tree fern: a comparison of linear and non-linear methods, *Water Res.*, 40 (2006) 119–125.
- [57] X. Yang, B. Al-Duri, Kinetic modeling of liquid-phase adsorption of reactive dyes on activated carbon, *J. Colloid Interface Sci.*, 287 (2005) 25–34.
- [58] Y.-S. Ho, G. McKay, Pseudo-second order model for sorption processes, *Process Biochem.*, 34 (1999) 451–465.
- [59] R.W. Peters, Chelant extraction of heavy metals from contaminated soils, *J. Hazard. Mater.*, 66 (1999) 151–210.